Int. J. Heat Mass Transfer. Vol. 6, pp. 425–443. Pergamon Press 1963. Printed in Great Britain.

SIMULTANEOUS HEAT AND MASS TRANSFER IN THE COMPRESSIBLE LAMINAR BOUNDARY LAYER OF A DISSOCIATING GAS

STEVEN IRWIN FREEDMAN† and JOSEPH KAYE‡

(*Received* 7 *May* 1962 *and in revised form* 4 *October* 1962)

Abstract—The velocity, temperature, and concentration profiles, the recovery factor, and the heat-transfer coefficient were calculated for the case of the supersonic flow of a dissociating diatomic gas (iodine vapor) over a flat plate without a pressure gradient. Results were obtained for various mass-transfer rates. Exact values of the thermodynamic and transport properties were used in order to compare the results with estimates based on constant property solutions where the reference enthalpy method is used to calculate the state at which the properties were evaluated.

NOMENCLATURE

c, mass fraction;
c_f, skin friction coefficient;
c_p, specific heat at constant pressure;
D, diffusion coefficient;
E, energy, intermolecular and dimensionless characteristic;
f, boundary layer stream function;
g_i, number of quantum states per energy level;
h, heat-transfer coefficient;
i, enthalpy;
K_p, equilibrium constant;
k, thermal conductivity;
k_B, Boltzmann's constant;
Le, Lewis number;
M, Mach number;
M_i, molecular weight of species i;
$\dot{m}$, mass flux;
Nu, Nusselt number;
Pr, Prandtl number;
p, pressure;
q, heat flux;
R, recovery temperature function;
R_g, gas constant;
Re, Reynolds number;
r, recovery factor;
St, Stanton number;
T, temperature, absolute;
t, temperature difference ratio;
U, free stream velocity;
u, X-direction velocity;
v, Y-direction velocity;
w, rate of production of a chemical species per unit volume;
x, co-ordinate parallel to the plate surface and the free stream;
y, co-ordinate perpendicular to the plate surface.
z, intermolecular distance;

Greek symbols

γ, ratio of specific heats;
Δ, difference between a quantity evaluated for species 1 and 2;
ϵ, depth of molecular energy well;
η, boundary layer co-ordinate;
θ, characteristic temperature;
λ, thermal conductivity of non-reactive gas mixture;
μ, absolute viscosity;
ν, kinetic viscosity;
ρ, mass density;
σ, collision diameter;
τ, shear stress;
ϕ, dissipation function;
ψ, stream function.

† Assistant Professor of Mechanical Engineering, M.I.T., Cambridge, Massachusetts, U.S.A.
‡ Late Professor of Mechanical Engineering, M.I.T., Cambridge, Massachusetts, U.S.A.

Subscripts

- ∞, free stream condition, used in dimensionless numbers;
- 0, stagnation condition for temperature and enthalpy;
- 1, monatomic gas property;
- 11, collision parameter for monatomic–monatomic collision;
- 12, collision parameter for monatomic–diatomic collision;
- 2, diatomic gas property;
- 22, collision parameter for diatomic–diatomic collision;
- Aw, adiabatic wall condition;
- e, equilibrium property;
- f, frozen state corresponding to nonreactive condition in an equilibrium mixture;
- i, enthalpy difference method;
- i, j, chemical constituents;
- p, constant pressure;
- T, temperature difference method.

Superscripts

- $\bar{}$, denotes dimensionless quantity obtained by dividing the free stream condition;
- *, reference enthalpy state;
- ′, differentiation with respect to η.

INTRODUCTION

THE PROBLEM of determining heat- and mass-transfer rates in dissociating gases has received considerable attention [1, 2, 3]. Much of the previous work has been based upon idealized models of the physical and chemical structure of the gas. The present investigation is concerned with establishing the extent to which these simplifications affect the accuracy of the computation of the overall transfer rates in a gas composed only of dissociating diatomic molecules. The present analysis is based on a model in which all properties of the gas are allowed to vary throughout the boundary layer and are computed using the most accurate methods presently available for the computation of thermodynamic and transport properties. The method used to determine the heat- and mass-transfer coefficients was to formulate the problem in terms of classical boundary layer theory, and to use the actual physical properties of the gas at each location in the boundary layer during the integration procedure. The calculations were for the case of local chemical equilibrium.

The study of a compressible boundary layer in a chemically reacting system with simultaneous heat- and mass-transfer is a natural continuation of classical boundary-layer theory. The development of the theory from the study of incompressible, constant property and constant pressure flows, to studies with all of these restrictions removed has resulted in a better understanding of the transport processes which occur in the boundary layer, and the development of powerful tools for further exploration. It is to be expected that when concentration gradients exist in the boundary layer, methods of solution based on constant values of the thermodynamic and transport properties of the gas will not be as accurate as methods in which these properties are permitted to assume their actual values. Recently Eckert [2] published a survey of boundary-layer heat-transfer knowledge, including the effect of mass transfer on the heat-transfer coefficient and the effect of chemical reactions on heat transfer. It contains 439 references to pertinent works which have appeared since the previous survey of 1956 [4]. Eckert [2] recommends basing heat-transfer computations on enthalpy differences rather than on temperature differences, and gives engineering formulae for the prediction of the heat-transfer rate in a dissociating gas based on an approximate method for evaluating properties.

Lees [3] has reviewed the progress made on the problems associated with the hypersonic boundary layer with simultaneous heat and mass transfer and with chemical reactions. Calculations of the heat-transfer coefficients have been made for two cases. In the case of local chemical equilibrium (infinitely fast reaction rate) solutions have been obtained with the assumptions of either zero mass-transfer rate or of the Lewis number equal to unity. In the case of frozen chemical composition (zero reaction rate) solutions have been obtained with the assumptions of constant specific heats and of the Prandtl, Lewis and Schmidt numbers and the $\rho\mu$ product

constant, for various values of the mass-transfer rate. These summaries, which are based on restrictions on the thermodynamic and transport properties of the gas mixture have permitted engineering estimates of heat transfer under varied conditions; however, the influence of these parameters away from their idealized values are of concern for the understanding of the accuracy of the transfer rates in the hypersonic boundary layer.

The present investigation examines the effects of mass transfer on a compressible laminar boundary layer in the presence of a dissociative chemical reaction. The model which was chosen was that of laminar supersonic flow over a flat plate, in the absence of a pressure gradient. The surface is assumed to be porous so that the gas can be forced through the wall at an appropriate rate.

Energy may be transferred through the boundary layer by either of two methods; by a temperature gradient causing a transport of the energies of molecular translation, rotation, and vibration, and by a concentration gradient causing a diffusive mass flux with an associated chemical energy transport. The diffusive energy flux which results from the mass flux is attributal to the difference of the chemical enthalpy levels of the counter-diffusing gases. These diffusive energy fluxes are independent of any thermal diffusion or other associated coupled energy and mass flux phenomena, which have been omitted from this analysis.

The problem is to prescribe the flow in terms of velocity, temperature, and concentration profiles throughout the boundary layer. In particular, the problem is to seek the influence of the mass-transfer rate on the recovery factor and on the heat-transfer coefficient.

ANALYSIS

The laminar compressible boundary-layer differential equations are:

Overall Continuity (Conservation of Mass)

$$\frac{\partial}{\partial x}(\rho u) + \frac{\partial}{\partial y}(\rho v) = 0. \tag{1}$$

Single Species Continuity (Conservation of the ith Chemical Species)

$$\rho\left(u\frac{\partial c_i}{\partial x} + v\frac{\partial c_i}{\partial y}\right) = \frac{\partial}{\partial y}\left(\rho D\frac{\partial c_i}{\partial y}\right) + w_i. \tag{2}$$

Motion, x-direction

$$\rho\left(u\frac{\partial u}{\partial x} + v\frac{\partial u}{\partial y}\right) = \frac{\partial}{\partial y}\left(\mu\frac{\partial u}{\partial y}\right). \tag{3}$$

Motion, y-direction

$$\frac{\partial p}{\partial y} = 0. \tag{4}$$

Energy

$$\rho\left(u\frac{\partial i}{\partial x} + v\frac{\partial i}{\partial y}\right) = \frac{\partial}{\partial y}\left(k\frac{\partial T}{\partial y}\right) + \mu\left(\frac{\partial u}{\partial y}\right)^2 + \sum_j \frac{\partial}{\partial y}\left(\rho D\frac{\partial c_j}{\partial y} i_j\right). \tag{5}$$

The above equations are to be solved for the case of an infinitely fast rate of chemical reaction; i.e. chemical equilibrium. Because we are considering a dissociating gas there are only two components, the monatomic and diatomic species. One single species continuity equation suffices to describe the composition. For this reason, the last term in the energy equation (5) is the sum of only two terms, and the diffusion coefficient D becomes the binary mixture diffusion coefficient.

When the above set of simultaneous nonlinear partial differential equations (1), (2), (3), and (5) are solved for the chemical equilibrium case, the local chemical composition is determined by the temperature and pressure, and is independent of the diffusion rates. Therefore, we need not consider the single species continuity equation, (2), any further. It is to be noted that the enthalpy, i, includes both the sensible and chemical energies. For a substance in local chemical equilibrium the enthalpy is uniquely determined.

It is assumed that boundary-layer approximations to the Navier–Stokes equations have a solution in which the velocity, temperature and concentration profiles at different x locations are of similar form. The physical variables are a function of a single similarity variable η. When the partial differential equations are transformed from the x–y plane to the x–η

plane, the variable x, and all derivatives taken with respect to x, vanish. The boundary conditions must be such that they permit similarity solutions. The transformation from the x–y plane to the x–η plane is as follows: The boundary-layer similarity co-ordinate η is defined as:

$$\eta \equiv \tfrac{1}{2}\sqrt{\left(\frac{U}{\nu_\infty x}\right)}\int_0^y \frac{\rho}{\rho_\infty}\,dy. \tag{6}$$

A stream function, ψ, is introduced, which identically satisfies the overall continuity equation

$$\rho u \equiv \frac{\partial\psi}{\partial y}, \qquad \rho v \equiv -\frac{\partial\psi}{\partial x}. \tag{7a, b}$$

The boundary-layer stream function, f, is introduced:

$$f \equiv \frac{\psi}{\sqrt{(\rho_\infty \mu_\infty U x)}} \tag{8}$$

where f is assumed to be a function of η only. The physical variables are transformed to a dimensionless variable by using the ratio of the actual variable to the free stream value of the variable. The boundary-layer ordinary differential equations expressed in boundary-layer co-ordinates are:

Motion, x-direction:

$$ff'' + (\bar{\rho}\bar{\mu}f'')' = 0. \tag{9}$$

Energy:

$$f\bar{c}_p\bar{T}' + \frac{1}{Pr_\infty}(\bar{\rho}\bar{k}\bar{T}')' + \frac{U^2}{2c_{p_\infty}T_\infty}\bar{\rho}\bar{\mu}f''^2 = 0. \tag{10}$$

The result of the transformation is a set of two coupled simultaneous non-linear, ordinary differential equations in two unknowns. Since the coefficients in these differential equations are also functions of the unknown variables, and since the equations are non-linear with mixed boundary conditions, a numerical integration technique was used to find the solutions to the differential equations.

PROPERTIES OF A DILUTE BINARY GAS

In order to solve the ordinary differential equations describing the convection and diffusion of energy and momentum, one must calculate the thermodynamic and transport properties of the gas in the boundary layer. The thermodynamic properties of a dilute gas have been extensively studied by the methods of statistical mechanics. The problem of calculating the thermodynamic properties involved determining the specific heats, over the temperature range from absolute zero to the maximum temperature encountered. The transport properties are more difficult, as the collision dynamics must be solved for all possible collision parameters and the results averaged over the velocity distribution. These collision interactions require knowledge of the interaction potential for all possible pairs of molecules. Appropriate mixing rules have been developed which enable us to compute the transport properties of the dilute binary gas.

The thermodynamic properties of a dilute binary gas, such as a mixture of monatomic and diatomic iodine, can be obtained from the properties of each species by use of the usual Gibbs–Dalton relationships. The thermodynamic properties of the components can be summarized by describing their specific heats. The monatomic component's specific heat at constant pressure is $5R_g/2$. If the gas is at a high enough pressure so that local chemical equilibrium accurately describes the gas, and also at high enough temperature so that appreciable dissociation occurs, then the diatomic species will be at a high enough temperature so that all the rotational quantum levels will be fully excited. The gas will probably be at a low enough temperature such that the vibrational modes of internal motion of the diatomic species will still require a quantum statistical computation for the vibrational contribution to the enthalpy. The specific heat at constant pressure of the diatomic species is therefore

$$\left[\frac{7}{2} + \frac{E^2e^E}{(e^E - 1)^2}\right] R_g.$$

The corresponding enthalpies are $5/2\,RT$ for the monatomic species and

$$\left(\frac{7}{2} + \frac{E}{e^E - 1}\right) R_g$$

for the diatomic species. The difference in enthalpies of the monatomic and diatomic

species at absolute zero must be taken into account in order to determine the enthalpy of reaction at any temperature. The zero point enthalpy difference was taken from the N.B.S. Tables [5]. The equilibrium constant, K_p, was calculated by equating the free energies of the two species.

Estimation of the transport properties of a dissociating gas presents a much more difficult problem. The few experimental results which are available for the transport properties of binary mixtures corroborate the theoretical predictions based on the kinetic theory of dilute gases. These computational methods require knowledge of the interaction potential between all pairs of colliding molecules. A two-parameter model of the interaction potential is the simplest one which can accurately predict the experimental observations. One parameter is needed to specify the size of the particle, and the other to specify the nature of the temperature dependence of the macroscopic transport property. A Lennard–Jones 6-12 model of the interaction potential is as accurate as any other model for the purposes of calculating transport properties, and was chosen because of the availability of tables of collision integrals.

$$E(z) = 4\epsilon\left[\left(\frac{\sigma}{z}\right)^{12} - \left(\frac{\sigma}{z}\right)^{6}\right]. \qquad (11)$$

The first approximation to the perturbation solution to the Boltzmann transport equation as presented by Hirschfelder, Curtiss and Bird [6], was used to calculate the viscosity, thermal conductivity and diffusion coefficient. The Eucken correction [6] was used to compute the thermal conductivity of the diatomic species which was used in the computation of the thermal conductivity of the gas mixture.

SELECTION OF IODINE AS THE WORKING FLUID

This analysis is applicable for any diatomic gas capable of being dissociated. The selection of iodine was based on the possibility of constructing an operating dissociated gas wind tunnel. The particular details of this study which relate to iodine are the molecular properties of the iodine gas. The molecular properties could be changed to those of oxygen, nitrogen, hydrogen, or any other diatomic gas. These properties include:

(a) σ_{ij}, the collision cross section between the ith and jth species. There are three cross sections in a dissociating diatomic gas, σ_{11}, σ_{12}, σ_{22}.

(b) ϵ_{ij}, the depth of the energy well which occurs during collisions of the ith and jth species. There are three energy wells, ϵ_{11}, ϵ_{12}, ϵ_{22}.

(c) M_1 and M_2, the molecular weights of the species.

(d) θ_R, θ_v, the characteristic dimensionless temperature associated with the rotational and vibrational internal degrees of freedom.

(e) g_j, the degeneracy of the electronic ground state (and any other electronic state with energy low enough so that at the temperatures in question an appreciable fraction of the molecules exists in these states).

Some of these properties, θ_R and g_j, affect the solution only through their influence on K_p, the equilibrium constant. Most of these molecular parameters, (a) through (e), are known for the other gases which are of interest [8]. Results for other gases can be obtained by a straightforward application of this method with the appropriate molecular parameters.

Results are given here only for iodine. Approximate estimates for other gases could be obtained by scaling the temperatures in such a manner that the dissociation reaction occurs at the appropriate level. Analyses similar to this one have been made for the stagnation-point heat-transfer rate in the absence of mass transfer and with simplified gas properties [9].

Re-entry vehicles require accurate knowledge of stagnation point heating. The designers of such vehicles have not concentrated as much on the details of the boundary layer along the vehicle. However, the reverse is true for skip-glide vehicles and rocket engines; that is, the boundary layer must be understood, and controlled, with great accuracy. It appears feasible that experimental studies can be conducted in a dissociated gas wind tunnel, at pressures of 0·1–0·001 atm and temperatures in the neighborhood of 1000°K to 1200°K.

In principle, one could determine the interaction potential for colliding atoms from the description of the atoms based on quantum mechanics. However, the state of the art of quantum mechanics is such that the mathematical difficulties associated with even the simple hydrogen and helium molecules are enormous, so that at present we can use quantum mechanics only as a qualitative guide in determining collision details. The gas mixture which is being considered is dissociating iodine. The outer electrons of the iodine atom are $4d^{10}$, $5s^2$, $5p^5$, which are the same as those of the xenon atom with a 5p electron removed. The electron bond which holds the iodine molecule together is a sharing of a pair of 5p electrons. For every collision of a pair of iodine atoms, the unpaired p electrons may have either symmetric or antisymmetric wave functions, and their electron spin vectors will align in either a parallel or an anti-parallel configuration. The electrodynamic forces between the unpaired p electrons are such that the interatomic force is attractive for only the symmetric wave functions of the 5p electrons with anti-parallel spins. Three out of four collisions will occur in such a manner that the two colliding atoms behave in a manner very similar to that of colliding xenon atoms, with one p electron missing, and these cannot chemically combine. The remaining quarter of the collisions will have the quantum conditions which permit chemical combination. One can represent three quarters of the collisions between iodine atoms by collisions between xenon atoms with a high degree of accuracy. The wave function for the atom–atom collisions for which the electron wave function is symmetric with anti-parallel electron spins is the wave function which describes the motion of the iodine atoms within the iodine molecule.

The collisions dynamics for such an interaction will be different from those of the majority of collisions in which the monatomic iodine can be well represented by xenon atoms. The actual particle trajectories during these collisions however have also been approximated by the collision of xenon atoms for lack of better information concerning the actual dynamics. In this manner, an approximation was made for the monatomic collisions which is adequate for three fourths of the atom–atom collisions and all of the atom–molecule collisions. This approximation is believed to be superior to a hard sphere model because even though the uncertainty in the size of the atom is the same in the present approximation and the hard sphere one, the present model predicts a more realistic temperature variation of the transport properties at elevated temperatures than a hard sphere model.

The numerical values of the depth of the energy well, and of the cross sections for I_2 and Xe (which we are using to approximate I), are taken from Hirschfelder's tabulation [6]

$$\sigma_{11} = 4{\cdot}055, \qquad \epsilon_{11}/k_B = 229,$$
$$\sigma_{22} = 4{\cdot}982, \qquad \epsilon_{22}/k_B = 550.$$

The "*mixing rules*" used in order to obtain the Xe–I_2 collision parameters are those based on the physical interpretation of the properties

$$\sigma_{12} = \frac{\sigma_{11} + \sigma_{22}}{2} \qquad \epsilon_{12} = \sqrt{(\epsilon_{11}\,\epsilon_{22})}$$

THE THERMAL CONDUCTIVITY OF A DISSOCIATING GAS IN LOCAL THERMODYNAMIC EQUILIBRIUM

In as much as energy is transported by both heat conduction and mass diffusion, the energy flux is the sum of two terms

$$\bar{q} = -\lambda \nabla T - \rho D \Delta i \nabla c. \tag{12}$$

When the gas is in local chemical equilibrium the concentration is determined by the pressure and temperature. The equilibrium constant, K_p, relates the pressure and concentration. For a dissociating diatomic gas, one obtains:

$$K_p(T) = \frac{4pc^2}{1 - c^2}. \tag{13}$$

By differentiation and use of the Van 't Hoff and perfect gas equation, one obtains for the constant pressure case

$$k = \lambda + \frac{\rho D \Delta i^2\, c(1 - c^2)}{\bar{R}_g^2 T^3} \tag{14}$$

where λ is the component of the thermal conductivity relating to the transport of the translational, rotational, and vibrational energies of

the molecules, and k is the actual thermal conductivity.

SOLUTION OF THE BOUNDARY LAYER DIFFERENTIAL EQUATIONS

In order to determine the heat- and mass-transfer rates and the skin-friction coefficient, one must obtain the values of the temperature, concentration and velocity gradients at the wall. The profiles of temperature, concentration and velocity are needed in order to obtain various integrated thicknesses, besides being useful in showing the nature of the effects of physical processes.

The energy transport differential equation contains three terms. Two of the three terms are linear in the temperature variable, and the third is independent of the temperature variable. The differential equation could be solved by the superposition of two solutions if the properties were independent of temperature. The homogeneous solution always represents the solution to the heat-transfer problem in the absence of dissipation, and the particular solution always represents the case of the adiabatic wall, when the boundary conditions are chosen appropriately. These two cases can be solved separately.

The dimensionless temperature function for the heat-transfer case is

$$\theta(\eta) = \frac{\bar{T}(\eta) - 1}{\bar{T}_w - 1}. \tag{15}$$

The dimensionless temperature function for the case of the adiabatic wall is

$$R(\eta) = \frac{\bar{T}(\eta) - 1}{\overline{U^2/2\, c_p T}} \tag{16}$$

with the boundary conditions $\theta = 1$ and $R' = 0$ at $\eta = 0$, and $\theta = R = 0$ at $\eta \to \infty$.

The two differential equations which were solved were:

$$f\bar{c}_p\theta' + \frac{1}{Pr_\infty}(\bar{\rho}\bar{k}\theta')' = 0 \tag{17}$$

representing the homogeneous solution, and

$$f\bar{c}_pR' + \frac{1}{Pr_\infty}(\bar{\rho}\bar{k}R')' + \bar{\rho}\bar{\mu}\frac{f''^2}{2} = 0 \tag{18}$$

representing the particular solution. Equations (17) and (18) were solved by use of a high-speed digital computer.

Because of lack of time only the two separate cases were solved. Since the coefficients in the differential equations are combinations of various properties and their derivatives, which are strong functions of temperature, superposition of solutions is not valid. The results presented here are for the two separate cases. The two cases were solved in temperature regions where the degree of dissociation changed considerably between the wall and the free stream. This selection was done in order to determine the extent to which the dissociation chemical reaction affects the temperature profiles and the associated heat-transfer rate. The temperature regions were also selected so as not to be so great that the effects of the undissociation regions at both ends of the dissociation range dominated the effects of the dissociation reaction. It is believed that since the heat-transfer cases which were solved existed at the same temperature levels as the adiabatic wall cases, the use of the heat-transfer coefficient which was thus obtained with the appropriate adiabatic wall temperature should be sufficient for many engineering purposes.

In light of the complexities of the functions describing the properties, which are in essence the variable coefficients in the boundary-layer ordinary differential equations, and of the nature in which the two differential equations are coupled, it was decided that it was impossible to obtain a closed form analytical solution. Hence the solutions to the differential equations were obtained by numerical integration on the I.B.M. 709 high speed digital computer at the MIT Computation Center. There are sufficient boundary conditions, three for the third order momentum equation and two for the second order energy equation. Since some conditions are known at the wall end, and others are known at the free stream end, a direct integration from the wall to the free stream is not possible.

The method used was an iterative one. Guesses were made concerning the unknown boundary conditions at one end (the wall) and an integration was performed, terminating at the free stream. In general, the integration generated

free stream boundary conditions which did not match those specified. The two trial estimates of the unknown wall boundary conditions were then individually perturbed, and the differential equations integrated again. Comparisons were made with the specified free stream boundary conditions. This procedure produced influence coefficients evaluating the effects of the perturbations of the wall boundary conditions on the generated free stream conditions. The correct wall boundary conditions were obtained by inversion of the matrix of the influence coefficients, producing the specified free stream boundary conditions. Since the differential equations are non-linear, and because only linear influence equations were obtained, several iterations were necessary in order to arrive at the correct wall boundary conditions.

PROPERTIES OF IODINE GAS

Figs. 1–5 show the properties of iodine gas in local chemical equilibrium. Calculations were made for the temperature range of 600–2400°K, at temperature increments of 25°K. Fig. 1 shows the equilibrium constant K_p, which has the dimension of atmospheres. In the temperature range from 800–2400°K the equilibrium constant goes from $10^{-4.5}$ to $10^{2.25}$ atm, indicating that the equilibrium gas mixture changes from the diatomic to the monatomic species quite rapidly. The curvature is due to the changing enthalpy difference between the two species. In the neighborhood of 1500°K the equilibrium constant changes by a factor of 10 for a temperature change of 260°K.

Fig. 2 shows the mass and mole fractions dissociated at various pressure levels. Dissociation occurs for a much smaller temperature change at the lower pressures than at the higher pressures.

Fig. 3 shows the Prandtl, Schmidt and Lewis† numbers for iodine gas at 0·1 atm. Two Prandtl and two Lewis numbers are shown, one set corresponding to values of the specific heat and thermal conductivity in which the actual value of the property in the gas at equilibrium is used, and one set in which these individual properties have been calculated for a non-reactive mixture of the monatomic and diatomic species at a composition corresponding to equilibrium. These properties calculated for states of chemical equilibrium have the subscript e, while those properties calculated for the frozen, non-reactive, mixture have the subscript f. Since the thermal conductivity and the specific heat do not enter into the Schmidt number, there is only one curve. The Schmidt number, and the Prandtl and Lewis numbers, based on a non-reactive mixture merely reflect that the gas changes from the monatomic to the diatomic species.

The equilibrium Prandtl number starts out at 600°K at a value of 0·76, dips down to a value of 0·55 at 1000°K, then climbs to a value of 0·95 at 1450°K, and finally settles down to a value of 0·67 at high temperature. These deviations from a constant value are attributed to the fact that in the reaction zone both the thermal conductivity and the specific heat are abnormally large; however, the thermal conductivity becomes large and returns to its normal value sooner than the specific heat does. These individual properties are shown in Fig. 3.

The equilibrium Lewis number goes towards

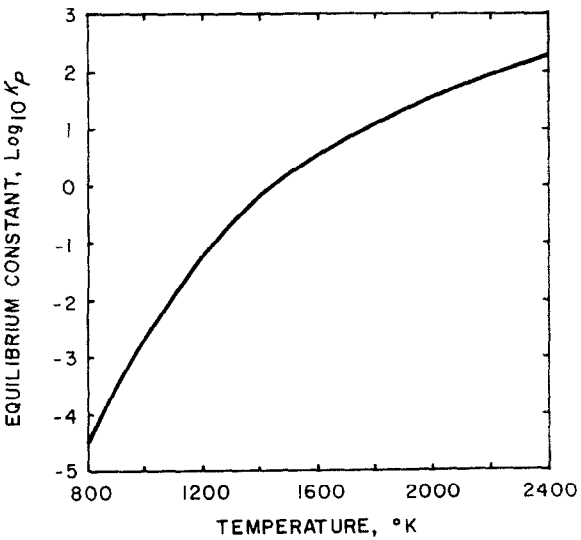

FIG. 1. The equilibrium constant of iodine gas.

† The Lewis number used here is $Le = \rho c_p D/k$ which is that used by Eckert [2], Lees [3], and Fay and Riddell [9]. The inverse form of the definition $k/\rho c_p D$, also appears in the literature.

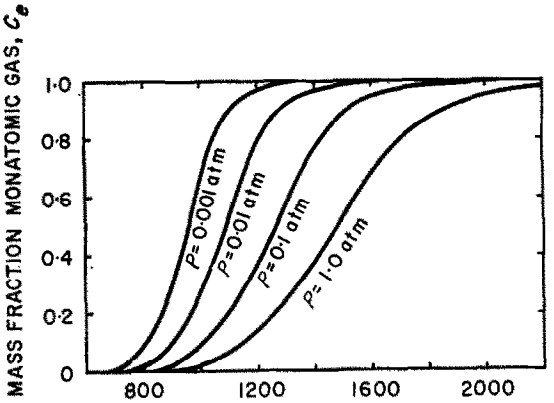

FIG. 2. The temperature variation of the fraction of iodine which is dissociated in a gas in equilibrium, for various pressures.

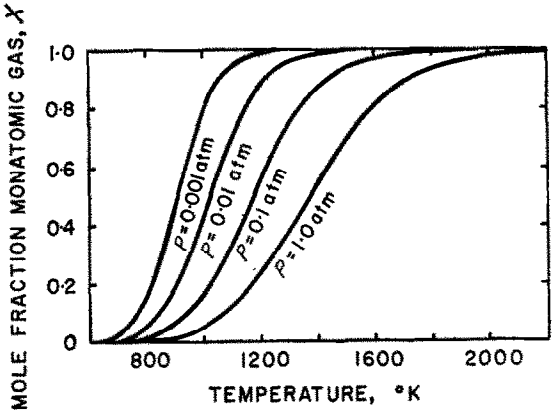

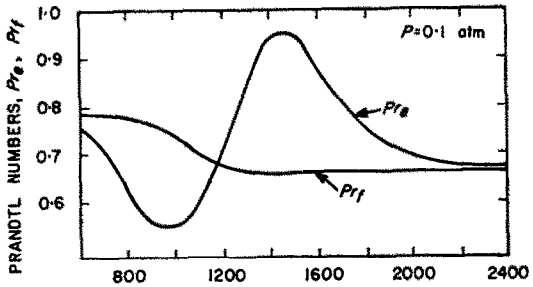

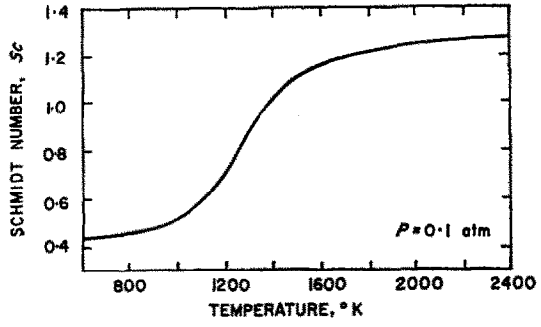

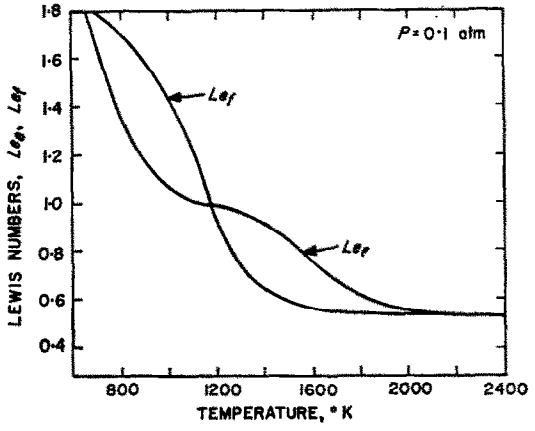

FIG. 3. Prandtl, Schmidt and Lewis numbers of iodine in dissociative equilibrium.

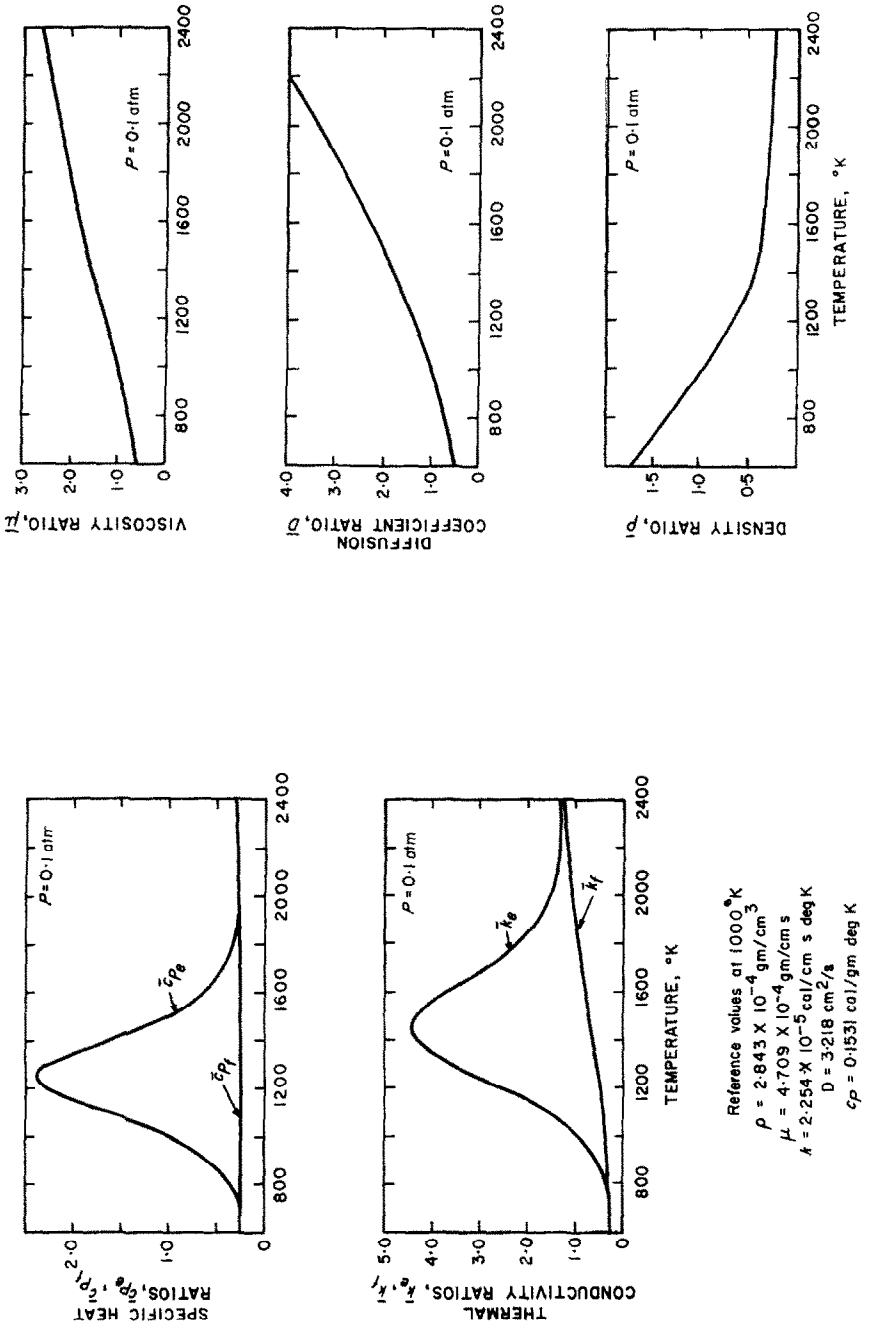

FIG. 4. Properties of iodine gas in chemical equilibrium.

unity very rapidly, and returns to the non-reactive value very slowly. This tendency of the Lewis number to go to unity in the reaction zone is because the incremental portion of the peaks of the specific heat and thermal conductivity due to dissociation and recombination are precisely in the ratio of $\rho D c_p : k$.

Fig. 4 shows the specific heat, thermal conductivity, viscosity, diffusion coefficient and density ratios over the temperature range from 600–2400 °K and 0·1 atm. All the curves have been normalized with respect to their values at 1000°K, which are tabulated in the figure. The viscosity and diffusion coefficient ratios are smooth curves. The density ratio shows the effect of dissociation. The non-reactive specific heat and thermal conductivity are also smooth curves. The equilibrium values of these properties show a large hump due to the presence of the large energy storage in the chemical bond.

Fig. 5 shows the enthalpy of the gas in equilibrium at various pressures. It is again seen that the change from diatomic to monatomic species occurs more rapidly at low pressures than at high pressures.

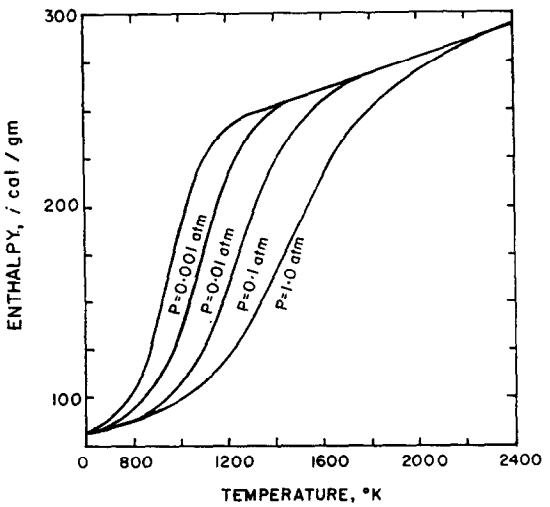

FIG. 5. Enthalpy–temperature diagram for iodine in equilibrium at various pressures.

HEAT-TRANSFER RESULTS

This section will describe the results for heat-transfer cases when the wall and free stream temperatures are specified as in Table 1. The heat transfer to the wall is:

$$q_w = -k_w \left(\frac{\partial T}{\partial y}\right)_w. \tag{19}$$

Obtaining the y derivative from the η derivative one evaluates the heat flux

$$q_w = -\frac{k_w \rho_w}{2}\left(\frac{U}{\rho_\infty \mu_\infty x}\right)^{1/2}\left(\frac{\partial T}{\partial \eta}\right)_{\eta=0}. \tag{20}$$

The numerical result of the computations for the heat-transfer case is the temperature gradient at the wall. Two solutions were obtained. One solution was with a free stream temperature of 1500°K, and the other was with a free stream temperature of 2000°K. In both cases, the wall temperature was one-half the free stream temperature; i.e. 750°K and 1000°K. The temperature gradients at the wall, for the solutions without mass transfer, are:

solution I, $T_\infty = 1500°K$, $T_w = 750°K$, $\bar{T}'_w = 0{\cdot}930$

solution II, $T_\infty = 2000°K$, $T_w = 1000°K$, $\bar{T}'_w = 0{\cdot}1688$

where $\bar{T}'$ is the derivative of the dimensionless temperature taken with respect to η. The η

Table 1. *Values of the wall boundary conditions*

Heat transfer case				
f_w	T_∞	T_w	$\bar{T}_w'$	f_w''
0	1500	750	0·930	0·920
−0·1	1500	750	0·866	0·834
−0·2	1500	750	0·797	0·752
0	2000	1000	0·1688	0·902
−0·1	2000	1000	0·1615	0·840
−0·2	2000	1000	0·1435	0·735

Adiabatic wall case					
f_w	T_∞	$T_{\infty,0}$	T_{Aw}	f_w''	r_T
0	1000	1274	1234	1·515	0·855
−0·1	1000	1274	1231	1·337	0·847
−0·2	1000	1274	1229	1·165	0·836
0	2000	3000	2877	1·315	0·877
−0·1	2000	3000	2856	1·173	0·856
−0·2	2000	3000	2835	1·026	0·835

derivative is related to the actual gradient at the wall by the equation:

$$\left(\frac{\partial T}{\partial y}\right)_w = \frac{\bar{\rho}_w}{2x}\sqrt{(Re_{x_\infty})}\,T_\infty \bar{T}'_w \qquad (21)$$

k_w and $\bar{\rho}_w$ are:

solution I,

$$\bar{\rho}_w = 3{\cdot}762,\ k_w = 0{\cdot}23624 \cdot 10^{-4}\ \frac{\text{cal}}{\text{cm s degK}},\quad p = 0{\cdot}1\ \text{atm}$$

solution II,

$$\bar{\rho}_w = 3{\cdot}653,\ k_w = 1{\cdot}3173 \cdot 10^{-4}\ \frac{\text{cal}}{\text{cm s degK}},\quad p = 0{\cdot}1\ \text{atm}.$$

Fig. 6 shows the mass flux, mass fraction of monatomic species, temperature and heat flux profiles for solutions I and II. The mass flux is almost a linear function of η from the wall to the edge of the boundary layer. The mass fraction of the monatomic species merely reflects the temperature profile, since the temperature fixes the concentration of the monatomic species.

The temperature and heat flux profiles shown in Fig. 6 are different from the profiles found in studies of boundary layers without chemical reaction. These anomalies are the result of the chemical reaction. In our case, in which a chemical reaction occurs in the boundary layer, the heat flux must supply the energy necessary to dissociate the gas in addition to supplying the energy which is transported to the wall. Therefore the heat flux must be largest in the vicinity of the reaction zone. Fig. 6 shows this maximum. Since the thermal conductivity is abnormally large in the reaction zone, the small temperature gradient in the central portion of the boundary layer, where the reaction is occurring, is to be expected. In the results for solution I ($T_\infty = 1500°\text{K}$, $T_w = 750°\text{K}$), it is noted that the

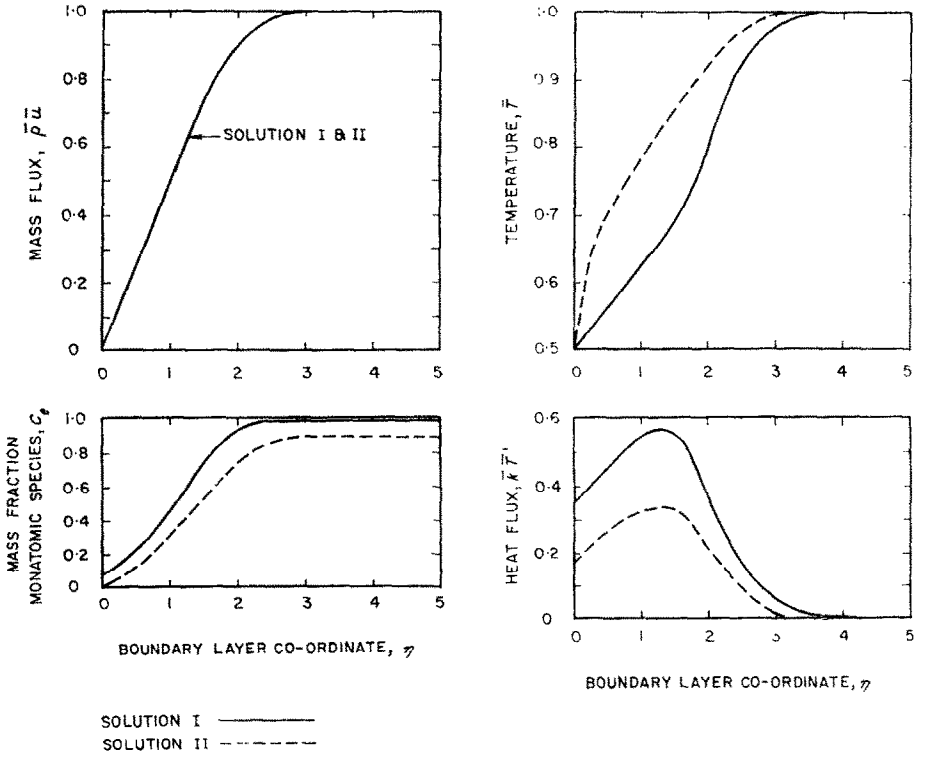

FIG. 6. Boundary-layer profiles of mass flux, mass fraction of monatomic species, temperature and heat flux, for the heat-transfer case.

gas is almost entirely undissociated near the wall, so that the thermal conductivity has a small value near the wall, and the temperature gradient is correspondingly high. However, in solution II ($T_\infty = 2000°K$, $T_w = 1000°K$), the wall is in the reaction zone, hence a high thermal conductivity and a small temperature gradient are found. These unusual temperature and heat flux profiles are one of the important results found during the course of this investigation.

ADIABATIC WALL RESULTS

This section describes the results obtained for the case of zero temperature gradient at the wall in the presence of dissipation. The problem is sometimes also referred to as the recovery factor case or the thermometer problem. It is the particular solution to the boundary-layer energy differential equation which includes the non-homogeneous dimensionless dissipation term

$$\phi = \frac{U^2}{2c_{p_\infty}T_\infty}\bar{\rho}\bar{\mu}\frac{f''^2}{2}. \tag{22}$$

When the specific heat is constant the factor $U^2/2c_{p_\infty}T_\infty$ is $M_0^2(\gamma_0 - 1)/2$, and is the difference between the dimensionless free stream stagnation temperature and the dimensionless free stream static temperature. In the case of variable specific heat the actual dissipation term, (22), is used.

During the process of integrating the ordinary differential equations the term $U^2/2c_{p_\infty}T_\infty$ appears only parametrically. In all the solutions which were calculated this parameter had the value of 0·5.

The stagnation enthalpy is given as:

$$i_{\infty\,0} = i_\infty + \frac{U^2}{2} \tag{23}$$

therefore

$$\frac{U^2}{2c_{p_\infty}T_\infty} = \frac{i_{\infty\,0} - i_\infty}{c_{p_\infty}T_\infty}. \tag{24}$$

$R(\eta)$ was calculated, where

$$R(\eta) = \frac{\bar{T} - \bar{T}_\infty}{(i_{\infty\,0} - i_\infty)/c_{p_\infty}T_\infty}. \tag{25}$$

$R(0)$, however, is not the recovery factor. The recovery factor, r, is

$$r_T = \frac{T_{Aw} - T_\infty}{T_{\infty\,0} - T_\infty}. \tag{26}$$

The stagnation temperature can be calculated since the stagnation enthalpy is determined by fixing the velocity parameter and the free stream temperature.

The local dimensionless temperature ratio

$$r_T(\eta) = \frac{T - T_\infty}{T_{\infty\,0} - T_\infty} \tag{27}$$

can now be calculated.

The enthalpy recovery factor can also be calculated:

$$r_i = \frac{i_{Aw} - i_\infty}{i_{\infty\,0} - i_\infty}. \tag{28}$$

The local dimensionless enthalpy ratio

$$r_i(\eta) = \frac{i - i_\infty}{i_{\infty\,0} - i_\infty} \tag{29}$$

can also be obtained by use of the enthalpy–temperature relationships.

Two solutions were calculated for the adiabatic wall case. These solutions are for the following physical cases:

solution III,

$$T_\infty = 1000°K, \frac{U^2}{2c_{p_\infty}T_\infty} = 0{\cdot}5, p = 0{\cdot}1 \text{ atm}$$

corresponding to a total temperature of 1274°K:

solution IV,

$$T_\infty = 2000°K, \frac{U^2}{2c_{p_\infty}T_\infty} = 0{\cdot}5, p = 0{\cdot}1 \text{ atm}$$

corresponding to a total temperature of 3000°K.

Fig. 7 shows the temperature difference ratio, total temperature, mass flux, mass fraction of monatomic species, enthalpy difference ratio, total enthalpy, temperature, and heat flux, for solutions III and IV. The mass flux profile shows an almost linear form near the wall, and blends into the free stream smoothly. The temperature, temperature difference ratio, and enthalpy difference ratio are also smooth curves, unlike the temperature profiles in the heat-transfer case. The temperature and enthalpy functions have smooth profiles in the

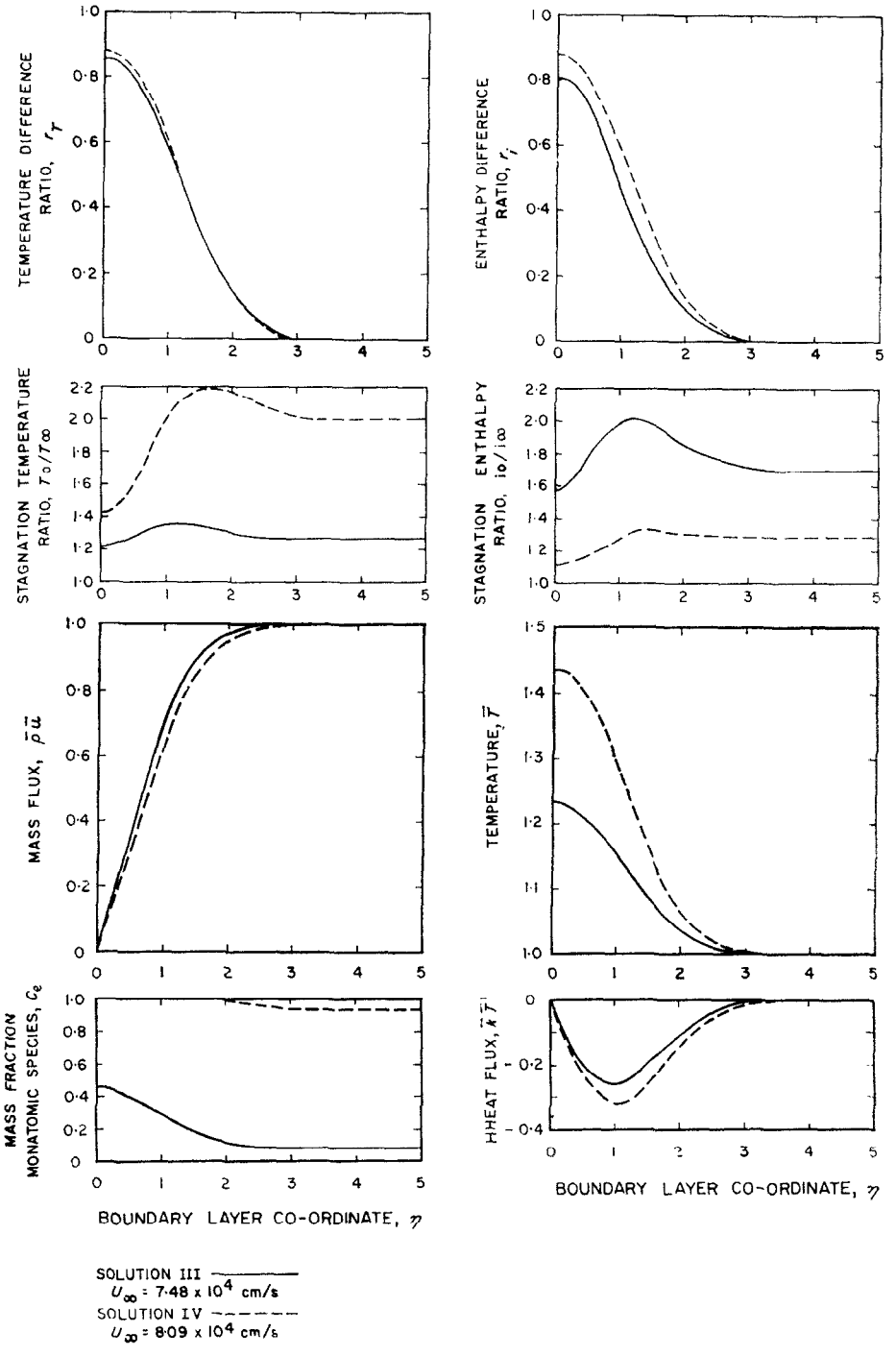

FIG. 7. Boundary layer profiles of temperature difference ratio, stagnation temperature, mass flux, mass fraction dissociated, enthalpy ratio, stagnation enthalpy, temperature and heat flux, for the adiabatic wall case.

adiabatic wall case because there is no net energy transport in such a boundary layer, only a conversion of kinetic into internal energy with a slight redistribution. A heat flux is only present in the central portion of the boundary layer which accounts for the redistribution of the energy. The dissipation is the source of energy transported by the heat flux. The heat flux is zero on both sides of the boundary layer because of the external, physical boundary conditions.

The temperature recovery factor found for solution III is 0·812. The enthalpy recovery factor in this case is 0·805. The free stream kinetic energy and the specific heat are very large, resulting in a small rise in the total temperature. Most of the free stream kinetic energy is used to increase the amount of gas dissociated.

The recovery factor found for solution IV is 0·877. In as much as the free stream is almost completely dissociated, there is no appreciable difference between the enthalpy definition and the temperature definition.

The effect of the chemical reaction is to increase both the specific heat and the thermal conductivity. There is a large thermal conductivity wherever there is a large specific heat. Since the Prandtl number does not vary more than 12 per cent from its free stream value of 0·67, we should expect the recovery factor (based on the temperature difference ratio) to be about 0·8. The temperature recovery factor is reasonably close to 0·8 in solutions III and IV. The variations are attributed to the unusual variations of the properties throughout the boundary layer.

EFFECT OF MASS TRANSFER

The effect of mass transfer on the heat-transfer coefficient can be given by the ratio of the heat-transfer coefficient with mass transfer to the heat-transfer coefficient without mass transfer. Heat-transfer coefficients were calculated for the same conditions as presented in the section on Heat-transfer results, except that there was a mass flux at the wall. This mass flux is:

$$(\bar{\rho}\bar{v})_w = -\frac{f_w}{2\sqrt{(Re_{x_\infty})}}. \tag{30}$$

Solutions were calculated for values of f_w of 0, −0·1, and −0·2.

Because the heat flux at the wall is

$$q_w = -k_w\left(\frac{\partial T}{\partial y}\right)_w \tag{31}$$

where the thermal conductivity is a function of temperature, the ratios of the heat-transfer coefficients are the ratios of the temperature gradients at the wall, for fixed T_∞ and T_w. These ratios of the heat-transfer coefficients are shown in Fig. 8. It is noticed that mass transfer has a bigger effect for the situation when $T_w = 750$ and $T_\infty = 1500$ than when $T_w = 1000$ and $T_\infty = 2000$. In the latter case the wall is hot enough for an appreciable amount of dissociation to be found at the wall. In a dissociation reaction two moles of the monatomic species are obtained for each mole of undissociating diatomic gas. The dissociation reaction results in a large decrease in density of the gas, thereby thickening the boundary layer. Thus a dissociating gas produces a "blocking effect" by thickening the boundary layer. When the wall is at a temperature, 1000–1500°K, there is a large concentration of the monatomic species near the wall, so that the portion of the boundary layer near the wall has already been thickened. This results in a smaller effect due to the additional thickening of the boundary layer by means of mass transfer when the gas at the wall is dissociated than when the gas at the wall is

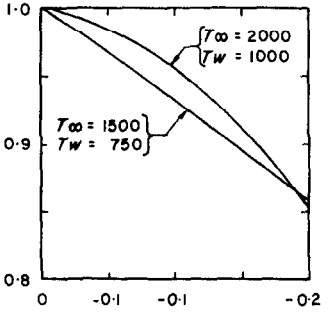

FIG. 8. Effect of mass transfer on the heat-transfer coefficient.

undissociated. When T_w is 1000°K and $f_w = -0{\cdot}2$, only a 3 per cent decrease in the heat-transfer coefficient is found, while when T_w is 750°K and $f_w = -0{\cdot}2$, a 15 per cent decrease is found.

Reductions in the recovery factor are shown in Fig. 9. It is seen that the recovery factor, like the heat-transfer coefficient, decreases with injection. The percentage decrease in the

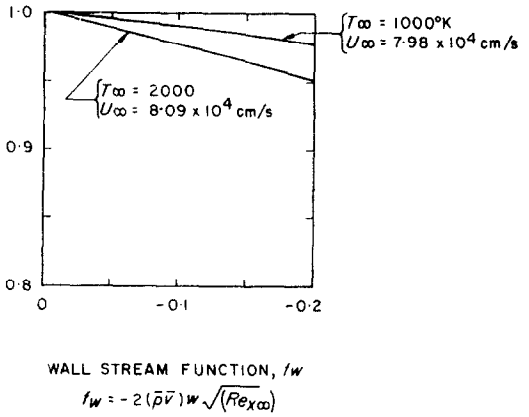

FIG. 9. Effect of mass transfer on the recovery factor.

recovery factor in the situation where dissociation is occurring at the wall is less than when there is no dissociation occurring at the wall. The value of the recovery factor itself is smaller when the wall is in the reaction zone. These two numerical results and the numerical results for the heat-transfer case are understandable in terms of the effect of the increase in specific volume of the gas accompanying dissociation.

FRICTION FACTOR

The shear stress on the surface of the plate is:

$$\tau_w = \mu_w \left(\frac{\partial u}{\partial y}\right)_w. \tag{32}$$

The friction factor is defined as:

$$c_f \equiv \frac{2\tau_w}{\rho_\infty v^2} = \frac{2\mu_w}{\rho_\infty v^2}\left(\frac{\partial u}{\partial y}\right)_w. \tag{33}$$

The velocity is given by:

$$\bar{\rho}\bar{u} = f'/2. \tag{34}$$

The y derivatives are related to η derivatives as

$$\frac{\partial}{\partial y} = \frac{\bar{\rho}}{2x}\sqrt{(Re_{x_\infty})}\frac{\partial}{\partial \eta}. \tag{35}$$

Combining terms to get the friction factor, one obtains:

$$c_f = \frac{\bar{\rho}_w \bar{\mu}_w}{2(Re_{x_\infty})^{1/2}}\left(\frac{f'}{\bar{\rho}}\right)_w'. \tag{36}$$

$\bar{\rho}'$ can be related to $\bar{T}_w'$ by use of the equations of state. f_w'' is included in the tabulated results given in Table 1.

CONCLUSIONS

In this section the exact value of the heat-transfer coefficient as obtained with the aid of the digital computer is compared with the value obtained by use of previously available approximate techniques. The best general technique available today is that of using the enthalpy difference as the driving potential, and evaluating the properties appearing in the dimensionless numbers at a reference enthalpy level [2]

$$q_w = h_i(i_{Aw} - i_w). \tag{37}$$

In this technique one uses the value of the specific heat calculated for the fictitious condition in which the composition of the gas corresponds to that of local chemical equilibrium, but in which the gas is considered to be a non-reactive mixture of its constituents, in evaluating the Nusselt number. The properties calculated for this frozen state are denoted by the subscript f. Properties calculated for the actual reactive mixture either have no subscript, or where a distinction is necessary, a subscript e is used.

This recommended form of the Nusselt number based on the enthalpy difference as the driving potential is:

$$Nu_i^* = \frac{h_i c_{p_f}^* x}{k_f^*}. \tag{38}$$

The asterisk indicates that the properties are to be evaluated at a reference enthalpy state:

$$i^* = i_\infty + 0{\cdot}5(i_w - i_\infty) + 0{\cdot}22(i_{Aw} - i_\infty). \tag{39}$$

An alternative form of the Nusselt number is based on the temperature difference as the

driving potential:

$$Nu_T^* \equiv \frac{h_T x}{k_e^*}. \tag{40}$$

It is desired that a method be found such that the Nusselt number is a unique function of the Reynolds number, Prandtl number, Lewis number and flow geometry, in order to have a simple method of predicting heat-transfer rates. Eckert suggests [2] that the equation (41) of Fay and Riddell [9] be evaluated at the reference enthalpy, and

$$Nu_i^* = 0{\cdot}332(Pr^*)^{1/3} \sqrt{(Re_x^*)} \left[1 - (Le_f^{*0{\cdot}52} - 1)\frac{\Delta i}{i_\infty}\right] \tag{41}$$

be used for the prediction of heat-transfer rates for a boundary layer flow when the gas is in local chemical equilibrium, the properties being variable. Such is the case under study. Using Eckert's preferred method, $Nu_i^*/\sqrt{(Re_x^*)}$ was calculated from the exact solution from the computer and was compared with $0{\cdot}332(Pr^*)^{1/3}$. $Nu_T^*/\sqrt{(Re_x^*)}$, $Nu_i^*/\sqrt{(Re_{x_\infty})}$ and $Nu_T^*/\sqrt{(Re_{x_\infty})}$ were also calculated. The Nusselt numbers were obtained from the exact solution by use of the following equations:

$$\frac{Nu_i^*}{\sqrt{(Re_x^*)}} = \frac{k_{we}}{k_f^*}\frac{\tilde{\rho}_w c_{p_f}^* T_w'}{2\Delta i}\sqrt{\left(\frac{\nu^*}{\nu_\infty}\right)} \tag{42}$$

$$\frac{Nu_T^*}{\sqrt{(Re_x^*)}} = \frac{k_{we}\tilde{\rho}_w T_w'}{k_e^* 2\Delta T}\sqrt{\left(\frac{\nu^*}{\nu_\infty}\right)}. \tag{43}$$

Since Le_f^* was 0·94 and 0·91 in the situations examined, the effect of the term

$$[1 - (Le_f^{0{\cdot}52} - 1)\,\Delta i/i_\infty]$$

was only 2–3 per cent.

Table 2 shows the comparisons of the various dimensionless numbers.

The enthalpy potential–reference method predicts a Nusselt number which is 14 per cent higher in one instance and 7 per cent lower in the other instance. The other method, the temperature potential method, predicts Nusselt numbers that are consistently low in comparison with our exact calculation. However, the temperature driving potential method, when used with the thermal conductivity calculated at the enthalpy reference condition, but using free stream property values in the Reynolds number, produces Nusselt numbers which agree to within 5 per cent with the variable property, but no chemical reaction case. The extent to which this is fortuitous remains uncertain until a sufficient number of solutions have been examined.

The best estimate of the recovery factor for laminar flow over a flat plate is that the recovery factor equals the square root of the Prandtl number:

$$r = \sqrt{Pr}. \tag{44}$$

The solutions obtained by having the digital computer locate the wall temperature at which the temperature gradient at the wall is zero gave the values shown in Table 3.

The computed results are in excellent agreement with the square root of the Prandtl number rule. There is only a small, 5 per cent, difference between the temperature recovery factor and the enthalpy recovery factor.

EFFECTS OF MASS TRANSFER

The only studies which have been made of the effect of mass transfer on heat transfer have been for either non-reactive gases, or for simplified property irreversible chemical reaction conditions (flames). For these cases with the properties dependent on temperature and concentration, Eckert [2] recommends that the effect of mass transfer on the heat-transfer

Table 2. Comparison of the dimensionless heat-transfer coefficient

T_w	T_∞	$Nu_i^*/\sqrt{(Re_x^*)}$	$Nu_i^*/\sqrt{(Re_{x\infty})}$	$Nu_T^*/\sqrt{(Re_x^*)}$	$Nu_T^*/\sqrt{(Re_{x\infty})}$	$0{\cdot}332(Pr^*)^{1/3}$
750	1500	0·336	0·480	0·193	0·276	0·290
1000	2000	0·273	0·465	0·171	0·290	0·291

Table 3. Recovery factors

T_∞	$T_{\infty 0}$	T_{Aw}	r_T	r_i	$\sqrt{Pr^*}$
1000	1274	1234	0·855	0·812	0·835
2000	3000	2877	0·877	0·877	0·820

coefficient be calculated using the following equation for laminar flow over a flat plate with no pressure gradient:

$$\frac{h}{h_{\dot{m}=0}} = 1{\cdot}0 - 0{\cdot}73\frac{\dot{m}}{\rho^* U}\frac{1}{St^*_{\dot{m}=0}}\left(\frac{M_\infty}{M_{inj}}\right)^{1/3}. \quad (45)$$

Eckert's form of the expression, (45), for the effect of mass transfer on the heat-transfer coefficient is an alternative to the expression of Gross, Hartnett, Masson, and Gazley [10]

$$\frac{q}{q_{\dot{m}=0}} = 1{\cdot}0 - 1{\cdot}82\left(\frac{M_\infty}{M_{inj}}\right)^{1/3}\left(\frac{\dot{m}}{\rho_\infty U}\right)\sqrt{(Re_x/C^*)} \quad (46)$$

where $C^* = (\rho\mu)^*/(\rho\mu)_\infty$. (47)

The expressions for the effect of mass transfer on heat transfer, (45) and (46), are empirical expressions arrived at by the correlation of many exact solutions obtained from analytical and numerical solutions to the boundary layer differential equations. These expressions may in the future become more general by evaluating the reference condition at a reference enthalpy and composition.

The results of Eckert's method are compared with the exact values for the present case obtained by solving the boundary layer energy differential equation for various mass-transfer rates. The comparisons are given in Table 4.

Table 4. Effect of mass transfer on the heat-transfer coefficient

f_w	T_∞	T_w	Actual value calculated	Predicted values St_i^*	St_T^*
−0·1	1500	750	0·931	0·941	0·899
−0·2	1500	750	0·857	0·822	0·797
−0·1	2000	1000	0·959	0·936	0·867
−0·2	2000	1000	0·853	0·872	0·735

It is seen that use of a Stanton number based on enthalpy difference as the driving potential comes closer to predicting the exact results than use of a Stanton number based on temperature difference as the driving potential.

All of the solutions obtained to date show little effect of mass transfer on the recovery factor for realistic mass-transfer conditions with real gases. For the mass-transfer rates studied, previous prediction methods indicate that the recovery factor would be reduced by about 1 per cent for $f_w = -0{\cdot}1$ and about 2 per cent for $f_w = -0{\cdot}2$. The results found in the present study were of this order of magnitude. For $f_w = -0{\cdot}2$ the recovery factor decreased by 2·5 per cent. This agreement of a situation in which there is a chemical reaction is in excellent agreement with the accepted variable property non-reactive case.

Previous numerical solutions to a boundary-layer differential energy equation (stagnation point) have only been calculated with the variable transport properties related by constant Prandtl and Lewis numbers [9]. The present calculations have included the effect of the actual variations in these properties. It is noted in Fig. 4 that in the reaction zone the Prandtl number varies rapidly, and the Lewis number is very nearly unity. An artificial Lewis number in which the specific heat and thermal conductivity account for only the chemical energy (the difference between the actual property and the equilibrium composition non-reactive property) is unity. The contribution to the thermal conductivity and the specific heat attributable to the chemical energy available during the reaction is the major portion of the property throughout the reaction zone.

ACKNOWLEDGEMENTS

This research was conducted under the Office Ordnance Research Contract number DA-19-020-ORD-4709, and was supported in part by the M.I.T. Computation Center.

REFERENCES

1. T. VON KÁRMÁN, *Fundamental Equations in Aerothermochemistry*, AGARD, Combustion Colloquium, Liege, Belgium, 5–9 December (1955). *Selected Combustion Problems*, II, Butterworths Scientific Publications, London (1956).
2. E. R. G. ECKERT, Survey of boundary layer heat

transfer at high velocities and high temperatures. WADC Technical Report 59–624 (1960).
3. L. LEES, Convective heat transfer with mass addition and chemical reactions, Reprint from *Combustion and Propulsion, Third AGARD Colloquium*, pp. 451–498. Pergamon Press (1958).
4. E. R. G. ECKERT, Survey on heat transfer at high speeds. WADC Technical Report 54–70 (1954).
5. F. D. ROSSINI, D. D. WAGNER, W. H. EVANS, S. LEVINE and J. JAFFE, Selected values of chemical thermodynamic properties. Circular of the National Bureau of Standards, Circular 500, United States Government Printing Office, Washington, D.C. (February 1952).
6. J. O. HIRSCHFELDER, C. F. CURTISS and R. B. BIRD, *Molecular Theory of Gases and Liquids*. Wiley, New York (1954).
7. S. CHAPMAN and T. G. COWLING, *The Mathematical Theory of Non-Uniform Gases*. Cambridge University Press (1958).
8. E. W. WASHBURN, ed., *International Critical Tables of Numerical Data, Physics, Chemistry, ahd Technology*. National Research Council, McGraw-Hill, New York (1926).
9. J. A. FAY and F. R. RIDDELL, Theory of stagnation point heat transfer in dissociated air, *J. Aero. Sci.* **25**, 73 (1958).
10. J. F. GROSS, J. P. HARTNETT, D. J. MASSON and C. GAZLEY, JR., *Int. J. Heat Mass Transfer*, **3**, 198 (1961).

Résumé—Les profils de vitesse, de température et de concentration, le facteur thermique pariétal et le coefficient de transmission de chaleur ont été calculés dans le cas d'un écoulement supersonique de gaz diatomique dissocié (vapeur iodique) sur une plaque plane sans gradient de pression. Les résultats ont été obtenus pour différents taux de transport de masse. On a utilisé les valeurs exactes des propriétés thermodynamiques et de transport pour comparer les résultats avec les estimations basées sur les solutions obtenues dans le cas de propriétés constantes; l'état pour lequel on évalue les propriétés est calculé par la méthode d'enthalpie de référence.

Zusammenfassung—Für Überschallströmung eines dissoziierenden, zweiatomigen Gases (Joddampf) ohne Druckgradient längs einer ebenen Platte wurden Geschwindigkeits-, Temperatur- und Kontrationsprofil, Rückgewinnfaktor und Wärmeübergangskoeffizient berechnet. Ergebnisse liessen sich für verschiedene Durchsatzmengen erhalten. Exakte Werte der thermodynamischen und der Transportgrössen dienten zum Vergleich mit Schätzungen, die auf Lösungen mit konstanten Stoffwerten beruhen, wobei der, den Stoffwerten zugrunde gelegte Zustand nach der Bezugsenthalpiemethode ermittelt wurde.

Аннотация—Проводится расчет профилей скорости, температуры и концентрации и коэффициентов восстановления и теплообмена для случая сверхзвукового течения диссоциирующего двуатомного газа (пары иода) на плоской пластине при отсутствии градиента давления. Данные получены для различных значений скорости переноса массы. Точные значения термодинамических свойств и характеристик переноса используются для сравнения этих данных с результатами, полученными из решений уравнений с постоянными характеристиками. При этом расчет уравнений состояния и термодинамических свойств производится методом исходной энтальпии.